Volume 24, No 4 | International Journal of Radiation Research, October 2026

Evaluation of a two-dimensional small field measurement array for stereotactic radiotherapy plan quality assurance

J. Gao[1#], H. Wei[2#], X. Nie[1], J. Yang[1], S. Zhang[1,3], H. Li[4], Z. Liang[1,2,3*]

[1]Cancer Center, Hubei Key Laboratory of Precision Radiation Oncology, Institute of Radiation Oncology, Union Hospital, Tongji Medical College, Huazhong University of Science and Technology, Wuhan, Hubei 430022, China
[2]Department of Radiotherapy, Affiliated Hospital of Hebei Engineering University, Hebei, China
[3]Key Laboratory of Biological Targeted Therapy (Huazhong University of Science and Technology), Ministry of Education, Wuhan, Hubei 430022, China
[4]Institute for Health Surveillance Analysis & Protection, Hubei Provincial Center for Disease Control and Prevention, Hubei, China

► ***Original article***

***Corresponding author:**
Zhiwen Liang, Ph.D.,
***E-mail:** 987542214@qq.com*

Received: July 2025
Final revised: April 2026
Accepted: June 2026

Int. J. Radiat. Res., October 2026; 24(4): 1175-1180

DOI: 10.61186/ijrr.24.4.31

Keywords: *Radiometry, quality assurance, stereotactic body radiotherapy, stereotactic radiosurgery.*

#These authors have contributed equally to this work.

ABSTRACT

Background: This study aimed to assess a two dimensional (2D) small field detector array for quality assurance (QA) in stereotactic radiotherapy (SRT), verify its key dosimetric properties, and evaluate its clinical performance for patient specific SRT plan verification. ***Materials and Methods:*** The myQA® SRS system comprises a 140 × 120 mm CMOS detector matrix with 400µm resolution, housed in a cylindrical ABS phantom. Tests included dose linearity, field size dependence, and beam angular response; clinical utility was validated via patient specific measurements. The detector's sensitivity to deliberately introduced MLC positional shifts was also examined by simulating systematic MLC offsets and comparing measured doses with planned values. ***Results:*** The basic characteristic test of the detector met the recommended specifications. The maximum deviation in detector signal relative to baseline readings was 0.5 %. The detector exhibited excellent dose linearity (R^2 = 1). Output factors agreed within 1.5 % compared with ionization chamber (IC) measurements for field sizes above 1 cm. Angular dependence was evaluated by comparing calculated and measured relative doses, and a lookup table (LUT) was established and validated. For clinical patient plans, the detector yielded an average gamma pass rate of 97.8 % ± 1.3 % under the 3 %/1 mm criterion. The detector was sensitive to systematic MLC offsets larger than 0.2 mm at 3 %/1 mm. ***Conclusion:*** The myQA® SRS detector is validated as a reliable tool for stereotactic radiotherapy plan QA, capable of providing high resolution real time dosimetric results.

INTRODUCTION

Ensuring the efficacy and safety of radiation therapy has always been a crucial concern in radiotherapy to decrease the severity and frequency of incidents. Implementing sophisticated radiation therapy techniques for patients while guaranteeing their precision and accuracy has important clinical consequences. The technicalities of radiation therapy have dramatically increased; While radiotherapy technology has advanced rapidly, supporting resources have not kept pace with rising workflow complexity [1].

Volumetric modulated arc treatment (VMAT) has become more prominent in delivering SRT [2,3]. SRT techniques involve providing precise targeted high dose treatment for small field dosimetry. The American Association of Physicists in Medicine (AAPM) Task Group No. 135 stated that "inaccurate estimates of accumulated dose as well as inaccurate estimates of the steepness" [4]. Dosimetric measurements for SRT, stereotactic radiosurgery (SRS), and stereotactic body radiotherapy (SBRT) are challenging due to small target volumes, which demand high precision and high-resolution QA devices [5,6].

Quality Assurance (QA) is a fundamental process designed to ensure the accurate deliverability of radiotherapy plans, serving as a critical safeguard for treatment safety and effectiveness [7,8]. Pretreatment patient specific quality assurance (PSQA) is a core component of treatment verification, and its importance has grown alongside the increasing complexity of modern radiotherapy, which requires stricter checks to reduce potential errors [9]. In clinical practice, 2D detector arrays are increasingly preferred for planar dose verification due to high efficiency and real-time readout [10,11]. However, their widespread application remains constrained by inherent limitations: point-dose measurements, often used with arrays, fail to capture full dose distributions, especially in regions with steep gradients [1, 5]. Radiochromic films offer superior spatial resolution but require specialized handling

[Downloaded from mail.ijrr.com on 2026-11-10]

[DOI: 10.61186/ijrr.24.4.31]

and lengthy processing, limiting their convenience in routine clinical workflows [5, 12]. There remains a strong clinical need for a QA device that combines high spatial resolution, a continuous active detection area, and accurate dose-map comparison, addressing limitations of current verification tools [13,14].

The myQA® SRS detector (IBA Dosimetry GmbH, Schwarzenbruck, Germany) is a high-resolution device designed for small-field PSQA. This study describes a comprehensive evaluation of the myQA® SRS detector to confirm its suitability for SRT plan QA and provide a practical reference for related clinical applications.

MATERIALS AND METHODS

This study includes a series of phantom measurements to determine the reliability of the myQA® SRS detector. We first performed tests of basic detector performance to confirm consistency with manufacturer specifications and clinical requirements. After commissioning, patient-specific plan verification was carried out. In addition, an MLC sensitivity study was performed to evaluate the array's ability to detect dose changes associated with MLC positional shifts.

The myQA SRS detector

Measurements were performed using a 2D myQA® SRS array, with data acquired and processed using myQA Patients software. The array uses a Complementary Metal-Oxide-Semiconductor (CMOS) solid-state design with 10,500 sensing elements, each measuring 0.4 mm × 0.4 mm, providing a spatial resolution of 0.4 mm. The active detection area is 12 cm × 14 cm. The array is embedded in an Acrylonitrile Butadiene Styrene (ABS) phantom (electron density = 1.06 g/cm^3) with a diameter of 19.3 mm. The myQA® SRS detector and cylindrical ABS phantom are shown in figure 1. Accurate phantom positioning was ensured using a precision digital level and alignment to the linac isocenter via the laser system. Acquired On-Board Imager (OBI) images were registered with the corresponding phantom CT images to confirm positioning accuracy.

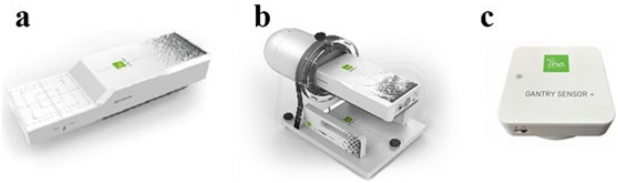


Figure 1. Overview of the myQA SRS detector: **(a)** myQA SRS detector array, **(b)** detector inserted in the cylindrical ABS phantom, **(c)** angle sensor unit.

Treatment unit and planning system

The plans were calculated in Eclipse version 15.6 (Varian Medical Systems, California, USA) treatment planning system using VMAT techniques with a 1 mm calculation grid. The number of arcs was based on the actual situation in individual treatment plans. The number of arcs was determined by the requirements of individual clinical plans. Radiation was delivered using a Varian Trilogy linear accelerator with a 6 MV flattening-filter (FF) beam. A dedicated CT scan of the myQA® SRS detector in its phantom was also acquired. The phantom was centered on the CT couch to ensure alignment between the measurement isocenter and the CT image center.

Basic characteristic test

Detector warm up and noise compensation

A precise protocol was followed to set up the system configuration and execute accurate exposure measurements under the manufacturer's guidelines [15]. A 30-minute warm-up period was applied before measurements to ensure stable output, as recommended. A background acquisition was performed before dose measurements to reduce residual electronic noise. Warm-up and noise compensation were applied at the start of every measurement session in preparation for plan verification.

Absolute dose calibration

The AAPM Task Group No. 218 recommended a dose calibration verification before each measurement session to factor in the daily variation of linac output [7]. Detector calibration was performed at the beginning of the study. The acquired CT images were imported into the TPS. The plan isocenter was matched to the center of the detector plane. Linac parameters were set as follows: gantry angle 0°, field size 10 cm × 10 cm, SAD = 100 cm, and 100 monitor units (MU). A fixed dose rate of 600 MU/min was used, consistent with routine clinical settings. The linac was calibrated and quality-checked before experiments. The detector was replaced with an ionization chamber insert for cross-calibration, and array readings were normalized against ionization chamber measurements.

Dose linearity and reproducibility test

The MU values were delivered from a minimum of 100 to a maximum of 600 to evaluate the linearity of myQA SRS dose response (gantry angle of 0°). The signal within the central 10 cm × 10 cm pixel region was recorded, and an MU-dose scatter plot was fitted to determine the coefficient of determination (R^2). For dose reproducibility, 100 MU was delivered five times under identical conditions, and the central signal was recorded each time.

Output factors

The linear accelerator parameters were set as follows: the gantry angle of 0° and 100 MU. The Field sizes ranged from 1 cm × 1 cm to 10 cm × 10 cm. Five repeated measurements were made for each field size, and the average value was used for output factor analysis. Identical measurements were repeated

[Downloaded from mail.ijrr.com on 2026-11-10]

[DOI: 10.61186/ijrr.24.4.31]

using an ionization chamber insert, and detector results were compared with ionization chamber measurements (after cross calibration).

Beam angular dependence

Obliquely incident beams passing through a 2D array travel different paths through diode structures and associated electronics, which can noticeably alter recorded signals. For myQA® SRS to be reliably used for VMAT plan verification, its angular response must be accurately characterized and corrected. A preliminary evaluation of angular dependence was performed, and an angular dependence lookup table (LUT) was generated. The procedure was as follows: doses at isocenter were calculated for various gantry angles and measured with myQA® SRS under identical conditions (10 cm × 10 cm field, 100 MU). Results were imported into myQA Patients to generate the LUT. An anglse sensor remained connected during measurements to enable real-time gantry angle registration and correction.

Plan QA verification

The practical application in clinical cases included both square field plans and patient specific treatment plans (including four head stereotactic radiosurgery plans and 3 lung tereotactic body radiation therapy plans), sample planning images is shown in figure 2. Clinical plans delivered to patients were verified by delivering the same beam geometry and MU values to the detector array. Measurements were performed in the coronal plane. Treatment plans were registered to the myQA® SRS phantom following routine procedures used with other pretreatment QA detectors, so that the isocenter of the patient plan coincided with the array center. The TPS recalculated and exported dose distributions. The AAA algorithm was used for single-field plans, and AcurosXB was used for VMAT plans, both with a 1-mm dose grid. Measured dose distributions were compared with TPS calculations to generate fluence maps and absolute dose differences. The evaluation was performed a global gamma analysis (threshold = 10 %) [7, 16].

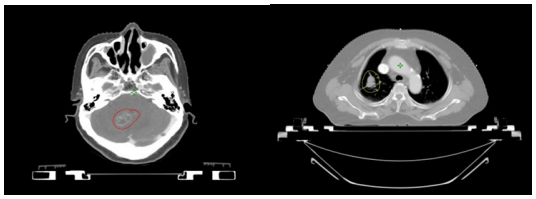


Figure 2. Representative treatment planning images for head and lung radiotherapy.

Sensitivity test of MLC offsets

Moreover, this study evaluated the sensitivity of the device to detect MLC systematic offsets that incorrect in the position of MLC. Systematic MLC opening or closing was simulated by symmetrically shifting both MLC banks (± 0.2 mm, ± 0.5 mm, ± 0.7 mm). Reference doses (no offsets) were compared with doses measured by the myQA® SRS detector with introduced offsets to assess dosimetric impact. All statistical analyses were performed using SPSS 20.0 (IBM, USA).

RESULTS

Basic characteristic test

As shown in figure 3, the results of the detector's performance showed dose linearity (R^2 = 1). Moreover, the dose reproducibility test showed that the maximum deviation of the detector readings was within 0.5 %. Figure 4 reports the output factors (OF) measurement of the detector. Diodes showed an over response with increasing beam field size, a behavior that was more significant for field size lower than 2 cm × 2 cm. The factors were within 1.5 % of the commissioning data acquired doses at 1000 mm SAD for field sizes from 2 cm to 10 cm, and factors were within 5% for 1 cm field size.

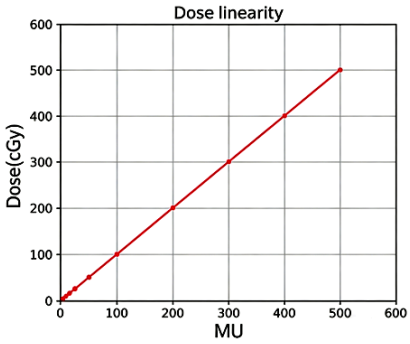


Figure 3. Dose linearity performance of the myQA SRS detector.

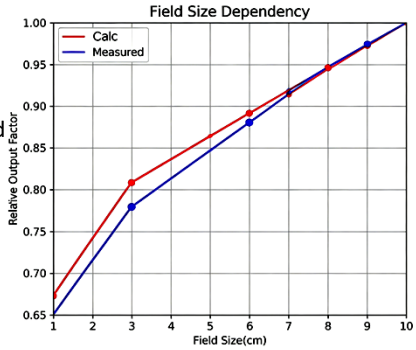


Figure 4. Output factors for different field sizes: measured values using the myQA SRS detector compared with TPS-calculated doses.

Figure 5 shows the variation of the detector response as a function of the incident beam angle. The data of all angles were found to have a mirror symmetry. The maximum difference at close to 90° / 270° that required significant corrections. Figure 6 presents the resulting plot of LUT as a function of gantry angle. Figure 7 reports the comparison of the relative dose calculated and measured with LUT correction as a function of the gantry angle (couch = 45°).

Plan QA verification

The single field (5cm×5 cm) results demonstrated the average gamma pass rates for calculated and measured dose comparison, were 100.0 % and 99.9

[Downloaded from mail.ijrr.com on 2026-11-10]

[DOI: 10.61186/ijrr.24.4.31]

% for 3 % /2 mm and 3 % /1 mm, respectively. Figure 8 demonstrates a dose distribution with a size of 4cm×4cm radiation field. Figure 8a is the field size set by the jaw (4cm×4cm), while figure 8b is the field size set by MLC (4cm×4cm) with a jaw size of 20cm×20cm, indicating the leakage dose distribution in the closed gap of the MLC. Figures 8c and 8d are obtained by zooming in figures 8a and 8b respectively, indicating the edge dose distribution of the MLC.

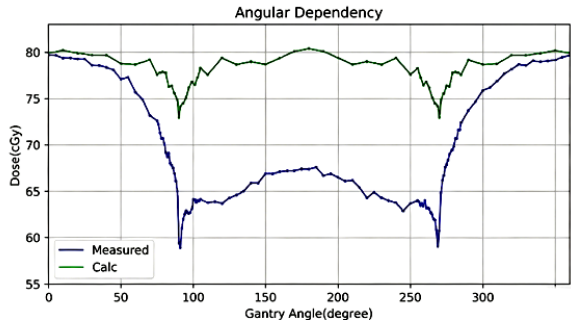


Figure 5. Beam angular dependence of the myQA SRS detector response.

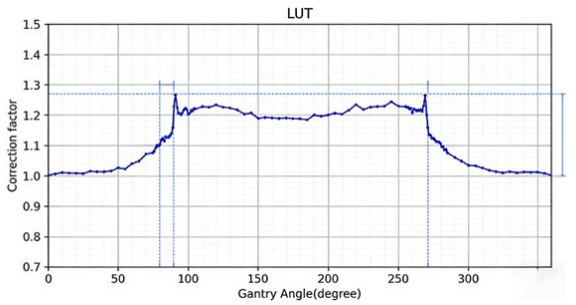


Figure 6. Look-up table (LUT) as a function of gantry angle.

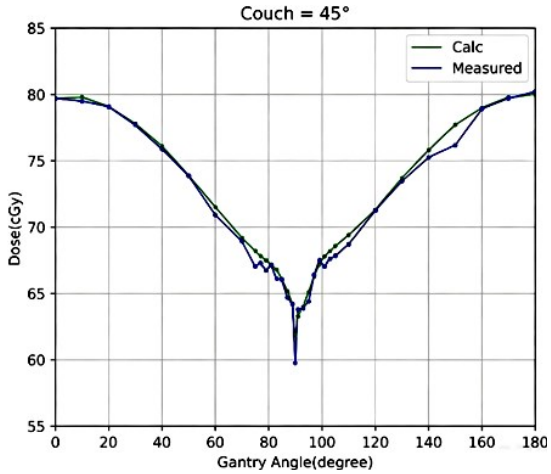


Figure 7. Comparison of calculated and measured relative doses with LUT correction at a couch angle of 45°.

Figures 9 and 10 show an example of the gamma analysis for a patient. Figure 9 shows the real time MLC movement during the plan measurement process. Figure 10a shows the dose distribution measured by myQA SRS detector, and Figure 10b demonstrates the dose distribution calculated. Figure 10c is the profile of calculated and measured, which shows a good agreement. Figure 10d presents the dose distribution difference of calculated and measured, and the gamma pass rates were 99.7 % for 3 % /1 mm by comparing calculated and measured.

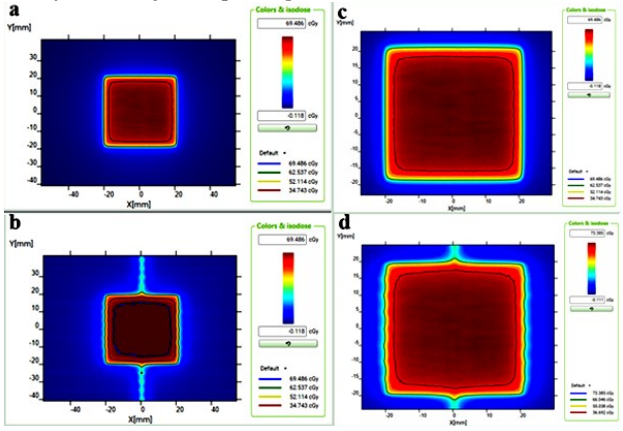
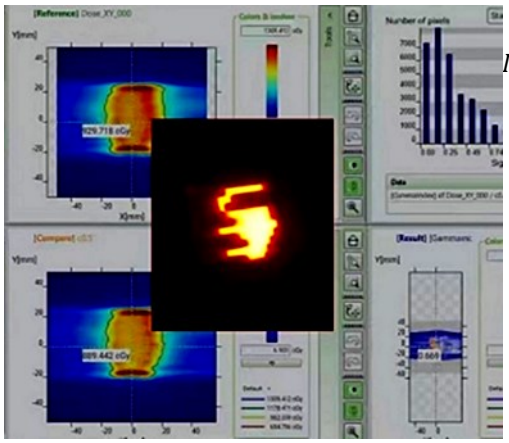


Figure 8. Dose distribution maps for a 4 cm × 4 cm square field: **(a)** field defined by jaws, **(b)** field defined by MLC, **(c)** magnified view of **(a)**, **(d)** magnified view of **(b)**.



MLC

Figure 9. Real-time motion status of MLC during patient-specific plan measurement.

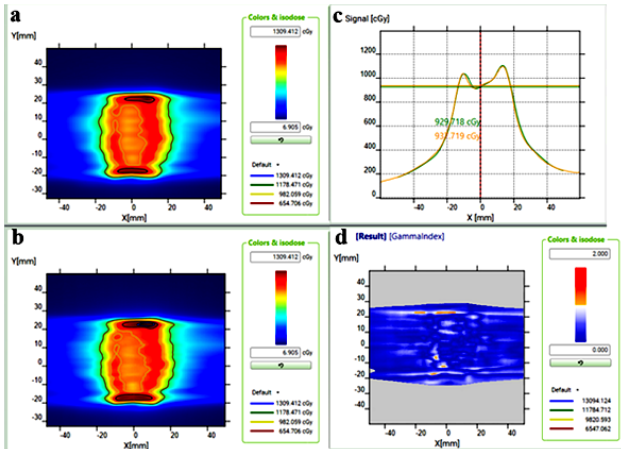


Figure 10. Results of patient-specific plan verification: **(a)** dose distribution measured by myQA SRS detector, **(b)** TPS-calculated dose distribution, **(c)** dose profiles of measured (green) and calculated (orange) distributions, **(d)** dose difference between calculation and measurement under the 3%/1 mm γ-analysis criterion.

offsets sensitivity tests

Table 1 and figure 11 show the mean gamma function results were obtained from the comparison the reference dose (without offsets) calculated and

[Downloaded from mail.ijrr.com on 2026-11-10]

[DOI: 10.61186/ijrr.24.4.31]

the measured dose introduced systematic MLC offsets for all plans. The mean gamma pass rates for all plans were 100 % ± 0.1 %, 99.8 % ± 0.15 % and 97.8 % ± 1.3 % for 3 % /3 mm, 3 % /2 mm, and 3 % /1 mm, respectively. 1 mm by comparing calculated and measured. The detector was sensitive to the greater than 0.5 mm introduced systematic MLC offsets using 3 % /3 mm and 3 % /2 mm gamma parameter, and it was sensitive to the greater than 0.2 mm using 3 % /1 mm gamma parameter. The gamma passes rates decreased significantly with increasing systematic MLC offsets.

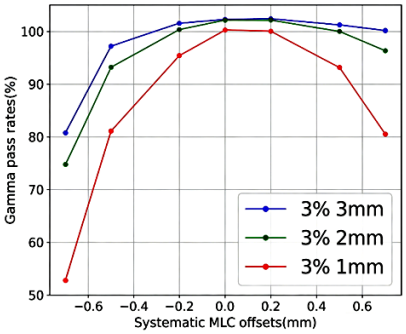


Figure 11. Mean γ pass rates between TPS-calculated reference dose (without offsets) and measured dose with systematic MLC positional offsets for all plans.

Table 1. Mean γ pass rates between TPS-calculated reference dose (without MLC offsets) and measured dose with systematic MLC positional offsets for all plans.

Plan types	3 % /3 mm	3 % /2 mm	3 % /1 mm
0.0 mm	100.0 %	99.8 %	97.8 %
- 0.2 mm	99.5 %	98.4 %	93.4 %
- 0.5 mm	95.6 %	91.6 %	79.2 %
- 0.7 mm	81.3 %	75.3 %	60.3 %
+ 0.2 mm	99.9 %	99.6 %	97.3 %
+ 0.5 mm	98.2 %	96.9 %	89.7 %
+ 0.7 mm	96.7 %	92.6 %	75.6 %

DISCUSSION

Patient plan verification is commonly performed using films, ionization chambers, or solid-state point arrays, each with distinct advantages and limitations for stereotactic radiotherapy QA [12, 17]. Stereotactic plans feature small targets and steep dose gradients, imposing strict requirements on QA detector accuracy and resolution [16]. Radiochromic films can achieve high-resolution dose measurements but are hindered by complicated, time-consuming operations and a high risk of errors [12], whereas the myQA SRS detector (a continuous high-spatial-resolution measurement detector developed by IBA) overcomes these limitations via efficient operation and real-time results, with no need for inter-element dose interpolation. This aligns with previous studies that have demonstrated 2D arrays as viable alternatives to films for dose verification [10, 11], as the myQA® SRS improves clinical efficiency while eliminating the practical drawbacks of film-based QA.

The myQA® SRS detector exhibited satisfactory basic dosimetric properties, including dose linearity, reproducibility, and output factors, all consistent with manufacturer specifications. These findings agree with published literature [18-20], which also reported reliable performance of the myQA® SRS detector and similar high-resolution devices for SRS/SBRT QA. Angular dependence is a key concern for 2D arrays in radiotherapy verification, but this issue was effectively managed using the manufacturer's recommended protocol: an angle sensor mounted on the gantry provides real-time angle and dose data during rotation. In terms of baseline performance, the myQA® SRS detector performed comparably to the widely used SRS Mapcheck array, as reported by the previous study [10], confirming its reliability as a QA tool. Gamma analysis is a standard method for patient-specific radiotherapy QA.

AAPM TG-218 recommends universal tolerance limits (gamma pass rate > 95 % at 3 % / 2 mm, 10 % threshold) for pretreatment PSQA of VMAT and IMRT plans using 2D arrays [7, 16]. For SRT plans, which are more sensitive to errors from MLC misalignment or setup uncertainty, some studies suggest using stricter 3 % / 1 mm criteria [13], a position supported by the present work. Our findings on gamma criteria for SRT QA are consistent with those studies that emphasize tighter tolerances to ensure stereotactic delivery accuracy [16, 21–23]. The myQA® SRS detector reliably identified discrepancies between delivered and calculated dose distributions, further supporting its clinical value for SRT plan verification.

Small MLC offsets can strongly affect plan delivery, making a QA detector's sensitivity to MLC shifts (particularly systematic offsets) a key performance metric for SRT QA. This study focused on the myQA® SRS detector's sensitivity to such offsets, with tests designed to reflect clinical conditions independent of plan complexity. The previous studies [10] confirmed that the comparable SRS Mapcheck 2D array could detect systematic MLC offsets ≥ 1 mm. Our results extend this observation: the myQA® SRS detector can detect systematic MLC offsets greater than 0.5 mm using 3 % / 1 mm criteria. This improved sensitivity is notable because many prior studies of MLC offset detection with commercial QA devices reported thresholds near 1 mm or larger [24–27], highlighting the improved ability of myQA® SRS to identify subtle MLC errors.

Consistent with Stepanek *et al.* [20], our study also suggests that the detector's ability to detect significant MLC positional deviations may depend on individual plan characteristics. Furthermore, we found that MLC offset sensitivity can be further improved by raising gamma pass thresholds (e.g., from 90 % to 95 %) or using stricter gamma criteria, consistent with optimization strategies in prior QA investigations [13,21]. The myQA® SRS detector's ability to visualize MLC error maps provides a useful tool for locating MLC positional errors, in agreement with the previous study [20], reinforcing its practical utility in clinical QA workflows.

[Downloaded from mail.ijrr.com on 2026-11-10]

[DOI: 10.61186/ijrr.24.4.31]

This study has limitations, including a relatively small number of patients and limited tumor sites. Future work will include a wider range of tumor sites and plan types (such as multi-target and non-coplanar plans) for more systematic analysis. Additional measurements will also be performed to investigate detector performance relative to target volume and plan complexity.

CONCLUSIONS

This study validates that the myQA® SRS detector is suitable and reliable for QA of SRT VMAT plans and supplies a practical reference for future clinical implementation. The detector also shows clear sensitivity to systematic MLC offsets that could produce clinically relevant dose deviations.

***Ethical approval and consent to participate*:** The Ethics Committee of Tongji Medical College, Huazhong University of Science and Technology gave a final approval (No.2016YFC0106702) for the study.

***Conflict of interest*:** The authors declare no conflict of interest.

***Funding statement*:** There are no funders to report.

***Authors' contribution*:** Z.L., Conception or design of the work; J.G., H.W. and H.L., data acquisition, analysis, or interpretation of data for the work; J.G. and H.W., drafting the manuscript or revising it critically for important intellectual content; Z.L., final approval of the version to be published; X.N., J.Y. and S.Z., contributions to all aspects of the work in ensuring that questions related to the accuracy or integrity of any part of the work are appropriately investigated and resolved.

REFERENCES

1. Huq MS, Fraass BA, Dunscombe PB, *et al.* (2016) The report of Task Group 100 of the AAPM: Application of risk analysis methods to radiation therapy quality management. *Med Phys, **43**(7): 4209-4262*.
2. Mayo CS, Ding L, Addesa A, *et al.* (2010) Initial experience with volumetric IMRT (RapidArc) for intracranial stereotactic radiosurgery. *Int J Radiat Oncol Biol Phys, **78**(5): 1457-1466*.
3. Wolff HA, Wagner DM, Christiansen H, *et al.* (2010) Single fraction radiosurgery using Rapid Arc for treatment of intracranial targets. *Radiat Oncol, **5**: 77*.
4. Dieterich S, Cavedon C, Chuang CF, *et al.* (2011) Report of AAPM task group 135: quality assurance for robotic radiosurgery. *Med Phys, **38**(6): 2914-2936*.
5. Halvorsen PH, Cirino E, Das IJ, *et al.* (2017) AAPM-RSS medical physics practice guideline 9. a. for SRS-SBRT. *J Appl Clin Med Phys, **18**(5): 10-21*.
6. Parwaie W, Refahi S, Ardekani MA, *et al.* (2018) Different dosimeters/detectors used in small-field dosimetry: pros and cons. *J Med Signals Sens, **8**(3): 195-203*.
7. Miften M, Olch A, Mihailidis D, *et al.* (2018) Tolerance limits and methodologies for IMRT measurement-based verification QA: recommendations of AAPM Task Group no. 218. *Med Phys, **45**(4): e53-e83*.
8. Ezzell GA, Galvin JM, Low D, *et al.* (2003) Guidance document on delivery, treatment planning, and clinical implementation of IMRT: report of the IMRT subcommittee of the AAPM Radiation Therapy Committee. *Med Phys, **30**(8): 2089-2115*.
9. Tiplica T, Dufreneix S, Legrand C (2020) A bayesian control chart based on the beta distribution for monitoring the two-dimensional gamma index pass rate in the context of patient-specific quality assurance. *Med Phys, **47**(11): 5408-5418*.
10. Banos-Capilla MC, Lago-Martin JD, Gil P, *et al.* (2021) Sensitivity and specificity analysis of 2D small field measurement array: Patient-specific quality assurance of small target treatments and spatially fractionated radiotherapy. *J Appl Clin Med Phys, **22**(10): 104-119*.
11. Popple RA, Sullivan RJ, Yuan Y, *et al.* (2021) Evaluation of a two-dimensional diode array for patient-specific quality assurance of HyperArc. *J Appl Clin Med Phys, **22**(12): 203-210*.
12. Niroomand-Rad A, Chiu-Tsao ST, Grams MP, *et al.* (2020) Report of AAPM task group 235 radiochromic film dosimetry: an update to TG-55. *Med Phys, **47**(12): 5986-6025*.
13. Rose MS, Tirpak L, Van Casteren K, *et al.* (2020) Multi-institution validation of a new high spatial resolution diode array for SRS and SBRT plan pretreatment quality assurance. *Med Phys, **47**(7): 3153-3164*.
14. Zhou Y, Liu Y, Chen M, *et al.* (2024) Commissioning and clinical evaluation of a novel high-resolution quality assurance digital detector array for SRS and SBRT. *J Appl Clin Med Phys, **1**: e14258*.
15. IBA Dosimetry (2022) myQA user's guide. IBA dosimetry; 2022. Available from: *https://www.iba-dosimetry.com*.
16. Xia Y, Adamson J, Zlateva Y, *et al.* (2020) Application of TG-218 action limits to SRS and SBRT pre-treatment patient specific QA. *J Radiosurgery SBRT, **7**(2): 135-147*.
17. Lee YC and Kim Y (2021) A patient-specific QA comparison between 2D and 3D diode arrays for single-lesion SRS and SBRT treatments. *J Radiosurgery SBRT, **7**(4): 295-307*.
18. Padelli F, Aquino D, Fariselli L, *et al.* (2022) IBA myQA SRS detector for cyberKnife robotic radiosurgery quality assurance. *Appl Sci, **12** (15): 7791*.
19. Junis I, Yousif Y, Stensmyr R, *et al.* (2024) Comprehensive characterisation of the IBA myQA SRS Detector for SRS and SBRT patient specific quality assurance. *Phys Eng Sci Med, **1**: 11*.
20. Stepanek CJ, Haynes JA, Fletcher S (2023) Evaluation of a complementary metal oxide semiconductor detector as a tool for stereotactic body radiotherapy plan quality assurance. *Phys Image Radiate Oncology, **25**: 100418*.
21. James S, Al-Basheer A, Elder E, *et al.* (2023) Evaluation of commercial devices for patient specific QA of stereotactic radiotherapy plans. *J Appl Clin Med Phys, **24**(8): e14009*.
22. Yasui K, Saito Y, Ogawa S, Hayashi N (2021) Dosimetric characterization of a new two-dimensional diode detector array used for stereotactic radiosurgery quality assurance. *Int J Radiate Res*, 19:281-289.
23. Kunii Y, Tanabe Y, Higashi A, Nakamoto A, Nishioka K (2023) Effects of high-resolution measurements between different multi-row detectors on volumetric modulated arc therapy patient-specific quality assurance. *Int J Radiat Res, **21**(3): 413-419*.
24. Prentou G, Pappas EP, Prentou E, *et al.* (2022) Impact of systematic MLC positional uncertainties on the quality of single-isocenter multi-target VMAT-SRS treatment plans. *J Appl Clin Med Phys, **23**(8): e13708*.
25. Saito M, Sano N, Shibata Y, *et al.* (2018) Comparison of MLC error sensitivity of various commercial devices for VMAT pre-treatment quality assurance. *J Appl Clin Med Phys, **19**(3): 87-93*.
26. Heilemann G, Poppe B, Laub W (2013) On the sensitivity of common gamma-index evaluation methods to MLC misalignments in Rapidarc quality assurance. *Med Phys, **40**(3): 031702*.
27. Zhou Y, Liu Y, Chen M, *et al.* (2024) Commissioning and clinical evaluation of a novel high-resolution quality assurance digital detector array for SRS and SBRT. *J Appl Clin Med Phys, **1**: e14258*.

[Downloaded from mail.ijrr.com on 2026-11-10]

[DOI: 10.61186/ijrr.24.4.31]